UCRL-JRNL-228888

LAWRENCE
LIVERMORE
NATIONAL
LABORATORY

Laboratory Measurements of 3 --> 2 X-ray Line Ratios of F-like Fe XVIII and Ni XX

M. F. Gu, H. Chen, G. V. Brown, P. Beiersdorfer, S. M. Kahn

March 12, 2007

Astrophysical Journal

Disclaimer

Laboratory Measurements of $3 \rightarrow 2$ X-ray Line Ratios of F-like Fe XVIII and Ni XX

M. F. Gu[1], H. Chen[1], G. V. Brown[1], P. Beiersdorfer[1], and S. M. Kahn[2]

ABSTRACT

The intensity ratios of $3 \rightarrow 2$ emission lines of Fe XVIII and Ni XX were measured on the Livermore electron beam ion trap (EBIT-I) with a flat-field grating spectrometer. The results were compared with distorted-wave (DW) calculations obtained with the Flexible Atomic Code and recent close-coupling calculations using the R-matrix code. The measured $3s \rightarrow 2p/3d \rightarrow 2p$ ratios are about 20–40% higher than the theoretical values. When more extended configuration interaction is included in the DW theory, the agreement with the measurements improved slightly. At the beam energies of these measurements, no significant resonance contribution is expected to be present, and the discrepancies represent the uncertainties in the direct excitation cross sections.

Subject headings: atomic data — atomic processes — line: formation — X-rays: general

1. introduction

The spectroscopy of the Fe L-shell X-ray emission is an important diagnostic tool for electron temperature and density, and iron abundances. The emission lines are dominated by $3 \rightarrow 2$ transitions from Fe XVII–XVIV. Although theoretical predictions of these line intensities have improved substantially over recent years, they still disagree significantly with laboratory measurements and astrophysical observations for many key transitions. One of the most serious issues of existing theoretical models is that calculations have not been able to reproduce the observed Ne-like Fe XVII spectrum with an accuracy comparable to the statistical uncertainties of may grating observations obtained with *Chandra* and *XMM-Newton* (Behar et al. 2001; Xu et al. 2002), and earlier crystal spectrometer data from the

[1]University of California Lawrence Livermore National Laboratory, 7000 East Avenue, Livermore, CA 94550

[2]Department of Physics, Stanford University, Stanford, CA 94305

Sun (Parkinson 1975; McKenzie et al. 1980; Phillips et al. 1982). There are two problems with the Fe XVII line ratios. One is the 3C/3D ratio for the two $3d$-$2p$ transitions located near 15 Å. Theoretical predictions of this ratio have been consistently larger than astrophysical observations, leading to speculations that opacity effects may have suppressed the stronger 3C line (Saba et al. 1999). However, laboratory astrophysics measurements with electron beam ion traps (EBIT) at the Lawrence Livermore National Laboratory (LLNL) and tokmaks at the Princeton Plasma Physics Laboratory (PPPL) have demonstrated that this low 3C/3D ratio is also obtained in optically thin plasmas (Brown et al. 1998, 2001b,a; Beiersdorfer et al. 2001, 2004). Moreover, it has also been shown that this ratio is further reduced by line blending with Fe XVI satellite transitions (Brown et al. 2001b; Behar et al. 2001). Another problem with the Fe XVII spectrum concerns the ratio of $3s$-$2p$ (near 17 Å) to $3d$-$2p$ line intensities. This ratio is found to be significantly larger in astrophysical observations than most theoretical predictions (Phillips et al. 1999). Because $3s$-$2p$ transitions are affected by radiative cascades and resonance contributions to a larger degree, it has been assumed that the models of their intensities are more vulnerable to large uncertainties. However, LLNL EBIT measurements have again shown that this ratio is larger than theoretical calculations even in resonance-free energy regions (Beiersdorfer et al. 2002). Brown et al. (2006) have recently measured the formation cross sections of 3C and 3D lines of Fe XVII by normalization to radiative recombination (RR) emission using the Goddard Space Flight Center X-ray microcalorimeter and the LLNL EBIT-I electron beam ion trap, and demonstrated that theoretical cross sections of the 3C line have the largest error.

Similar problems with the $3s$-$2p$/$3d$-$2p$ line ratios of F-like Fe XVIII have also been observed in the *XMM-Newton* data of NGC 4636 (Xu et al. 2002). However, the recent cross section measurements of the strongest $3d$-$2p$ lines of Fe XVIII indicate that the disagreement with the theory is not as large as for the 3C line of Fe XVII (Chen et al. 2006). Unfortunately, the spectrometer used in that measurement did not cover the strong $3s$-$2p$ transitions at wavelengths larger than 15.6 Å. In this paper, we present the measurements of line ratios of all significant $3 \rightarrow 2$ transitions of Fe XVIII and its iso-electronic equivalent, Ni XX, at electron energies close to the ionization thresholds of the respective ion, where no resonant processes are expected to contribute to the line intensities. In §2, we discuss the details of our measurements and data analysis. The results and comparisons with various theoretical predictions are presented in §3. §4 gives a brief summary.

2. measurement and analysis

The experiment was carried out on the EBIT-I electron beam ion trap facility of the Lawrence Livermore National Laboratory using a high resolution flat-field grating spectrometer. The details of the LLNL EBITs can be found elsewhere (Levine et al. 1988). The calibration and performance of the grating spectrometer are described in Beiersdorfer et al. (2004). The beam energy was set at 1.4 keV for the Fe XVIII measurement, and 1.7 keV for the Ni XX measurement, after accounting for the space charge potential corrections. These energies are slightly above the ionization potentials of Fe XVIII and Ni XX. They were chosen to maximize the populations of the two ions under study and minimize those of the neighboring charge states. Iron and nickel were injected in the form of $(C_5H_5)_2Fe$ and $(C_5H_5)_2Ni$, i.e., bis(cyclopentadienyle)iron and nickel, respectively, using a differential gas injection system. The electron density in the trap was $< 10^{12}$ cm^{-3}, and considered to be in the low density coronal limit for Fe XVIII and Ni XX lines.

The recorded spectra of iron and nickel are shown as the black traces in Figure 1. The spectra are dominated by the Ne-like and F-like ions. The line labels shown in Figure 1 are those used in Brown et al. (1998) and Brown et al. (2002) for iron ions, and Gu et al. (2007) for nickel ions. For the nickel measurement, O-like lines exist in our spectrum. However, the Ni XX transitions of interest are not significantly affected by the O-like lines with the exception of F3, which has contributions from the relatively strong O2 line. The effects of blendings with O-like lines are taken into account in our analysis as described below. The wavelength scale was established using the laboratory wavelengths of Fe XVII–XVIII (Brown et al. 1998, 2002) and Ni XIX–XX (Gu et al. 2007) lines. We assume Gaussian line shapes in the spectral fitting. The width of the line profiles are allowed to vary linearly with the wavelength, and the parameters are determined by fitting a few isolated lines across the wavelength range.

Some of the Fe XVIII and Ni XX lines have multiple components, and many have contributions from several weak lines. In the case of the nickel measurement, O-like transitions may also contribute to the Ni XX line intensities. To accurately account for these blends, we use a two-step fitting procedure to extract F-like line intensities. In the first step, we construct theoretical models using the Flexible Atomic Code (FAC, Gu 2003) for Ne-like, F-like, and O-like ions under mono-energetic electron excitation conditions. In these calculations, we include configuration interaction effects within all $n = 2$ and $n = 3$ configurations of respective ions. Because the photons are detected in the direction perpendicular to the electron beam, an anisotropic correction factor is also calculated and included in the analysis. The correction factors are typically less than 10%, and uncertainties associated with them are assumed to be negligible. The measured spectra are then fitted with theoretical models adjusting only the populations of Ne-like, F-like, and O-like ions. For the iron spectra, no O-like lines are detected, and the O-like abundance is fixed at zero. In the second step, we fix the ion abundances derived in the first step but vary the intensities of strong lines of Fe XVIII and Ni XX labeled in Figure 1 during the spectral fitting. For unresolved lines, such as the F5+F6 complex, the F13+F14+F15 complex, and the F17+F18 complex, the intensity ratios of the sub-components are fixed at the theoretical values, and only total intensities of the entire complex is reported. The F19 and F20 lines of Fe XVIII are well resolved in our measurement, while the corresponding lines of Ni XX are marginally resolved. In the analysis of nickel data, we also fix the ratio of F19 to F20 according to the FAC calculations. The results of spectral fitting in the second step are shown as red traces in Figure 1. The purpose of this two step procedure is to determine appropriate contributions of weak lines to the intensities of strong lines under investigation according to theoretical calculations.

3. results and discussions

The measured intensities of Fe XVIII and Ni XX lines are normalized relative to the F20 line, and shown in Table 1 and Table tab:Ni, respectively. The F20 line is the strongest line in the F-like spectra. It is comprised of two unresolved transitions from $1s^22s^22p_{1/2}2p^3_{3/2}3d_{3/2}(J = 5/2,3/2)$ levels to the $1s^22s^22p^2_{1/2}2p^3_{3/2}(J = 3/2)$ level in the jj-coupling notation, or equivalently, in the LS-coupling notation, from the $1s^22s^22p^43d(^2D_{5/2},^2P_{3/2})$ levels to the $1s^22s^22p^5(^2P_{3/2})$ level. This line can be considered to be the equivalent of 3C in the Ne-like spectra. The quoted uncertainties are the combination of statistical and systematic errors at the 1σ confidence level. The systematic uncertainties mainly arise from the spectrometer response, and are assumed to be 10% across the covered wavelength range. This estimate is based on the spectrometer response calibration performed using H-like and He-like Rydberg series of Ne, F, and O ions (Beiersdorfer et al. 2004). The statistical uncertainties are determined according to the total number of X-ray counts in each line complex using Poisson statistics.

The column labeled "Theory A" in Table 1 and 2 are calculated with the FAC model described in the previous section. In order to investigate the effects of configuration interactions on the calculated line ratios, we performed a larger calculation including all $n \leq 7$ singly excitation configurations as well as $3l^2$, $3l4l'$, and $4l^2$ doubly excited configurations. The line ratios calculated with this model are referred to as "Theory B".

The discrepancies between measured and calculated line ratios are summarized in Figure 2. It is clear that both Fe XVIII and Ni XX data suggest that the theoretical intensities of F4, F5+F6, F8, F9, and F11 lines relative to F20 are underestimated. When compared with "Theory A" values, the discrepancies are largest for F4, F5+F6, and F8, reaching 30–40%.

These lines are all $3s$-$2p$ transitions. "Theory B" line ratios bring the calculated and measured values into slightly better agreement, but discrepancies remain at the 20% level. On the other hand, the measured intensities of the $3d$-$2p$ transitions, i.e., F13+F14+F15, F16, F17+F18, and F19, relative to that of F20 appear to agree with the theoretical values very well. The measured and calculated ratios for F1, F2 and F3 also agree with each other reasonably well. F1 of Fe XVIII and F3 of Ni XX are slightly overestimated in theory. However, F3 of Ni XX is severely blended with the O-like line, O2, of Ni XXI, which contributes about 30% to the total intensity of the feature. The possible over-correction of the O2 contribution may partly cause the discrepancy for F3 of Ni XX.

These measurements were carried out at electron energies where no resonant processes are expected to contribute significantly to the line intensities. The discrepancies between theoretical and experimental values therefore reflect the problems in the direct excitation cross sections. Brown et al. (2006) have shown that the $3s$-$2p$/$3d$-$2p$ ratio discrepancies of Fe XVII are largely due to the overestimation of the 3C line cross sections in various theoretical calculations. In Fe XVIII, the measured cross section for F20, i.e., the equivalent of 3C, is $5.6 \pm 0.8 \times 10^{-20}$ cm^2 (Chen et al. 2006) at electron energies of 1.35 and 1.46 keV. The theoretical cross section from "Theory A" is 6.1×10^{-20} cm^2, or about 10% higher than the measured values, and that from "Theory B" is 5.58×10^{-20} cm^2, which agrees very well with the measured values. This indicates that for Fe XVIII, the discrepancies in the $3s$-$2p$/$3d$-$2p$ ratios are mainly due to problems in the line formation cross sections of the $3s$-$2p$ transitions.

Desai et al. (2005) studied the Fe XVIII line ratios of the corona of Capella in detail using the *Chandra* grating spectrometers. The differential emission measure of Capella's corona is peaked near $T = 10^{6.8}$ K (Brickhouse et al. 2000; Gu et al. 2006). At such temperatures, resonance excitation and dielectronic recombination processes are expected to contribute to the Fe XVIII line intensities, especially to those of the $3s$-$2p$ transitions (Gu 2003). In Table 1, we list the Fe XVIII ratios in Capella measured by the *Chandra* medium energy grating (MEG) from Desai et al. (2005). Witthoeft et al. (2006) recently computed the Fe XVIII atomic data using R-matrix theory including all $n = 3$ and $n = 4$ target states. Their predicted line ratios with resonance excitation contributions are also listed in Table 1 for a plasma temperature of $T = 10^{6.8}$ K, and referred to as "Theory C". The effects of resonance excitation and contributions from dielectronic recombination processes to Fe XVIII have also been investigated by Gu (2003), and we show those predicted ratios in Table 1 for a temperature of $T = 10^{6.8}$ K as well, which are referred to as "Theory D". The observed ratio of F4, F5+F6, and F8 in Capella are larger than the present measurements, which indicates the importance of resonant processes. These Capella ratios are also larger than both "Theory C" and "D" values, which indicates the problems in the direct excitation theory, as suggested by the present measurements.

4. Summary

In summary, we have measured the Fe XVIII and Ni XX line ratios using the Livermore electron beam ion trap EBIT-I and a high resolution flat-field grating spectrometer, at electron energies where no significant resonant processes are expected. We have shown that the measured $3s$-$2p/3d$-$2d$ line ratios are smaller than theoretical calculations using the Flexible atomic code. These discrepancies are attributed to the problems affecting theoretical direct excitation cross sections. The observed $3s$-$2p/3d$-$2p$ line ratios of Fe XVIII in Capella's corona are larger than the present measurements, indicating the importance of resonant processes. The Capella ratios are also larger than two independent theoretical calculations of the $3s$-$2p$ transitions that include resonant processes, again indicating that there exist problems with the calculation of the direct excitation cross sections.

The work at the University of California Lawrence Livermore National Laboratory was performed under the auspices of the U.S. Department of Energy under Contract No. W-7405-Eng-48 and supported by NASA Astronomy and Physics Research and Analysis grant NAG5-5419 to Stanford University and LLNL.

REFERENCES

Behar, E., Cottam, J., & Kahn, S. M. 2001, ApJ, 548, 966

Beiersdorfer, P., Behar, E., Boyce, K. R., Brown, G. V., Chen, H., Gendreau, K. C., Gu, M.-F., Gygax, J., Kahn, S. M., Kelley, R. L., Porter, F. S., Stahle, C. K., & Szymkowiak, A. E. 2002, ApJ, 576, L169

Beiersdorfer, P., Bitter, M., von Goeler, S., & Hill, K. W. 2004, ApJ, 610, 616

Beiersdorfer, P., von Goeler, S., Bitter, M., & Thorn, D. B. 2001, Phys. Rev. A, 64, 032705

Brickhouse, N. S., Dupree, A. K., Edgar, R. J., Liedahl, D. A., Drake, S. A., White, N. E., & Singh, K. P. 2000, ApJ, 530, 387

Brown, G. V., Beiersdorfer, P., Chen, H., Chen, M. H., & Reed, K. J. 2001a, ApJ, 557, L75

Brown, G. V., Beiersdorfer, P., Chen, H., Scofield, J. H., Boyce, K. R., Kelley, R. L., Kilbourne, C. A., Porter, F. S., Gu, M. F., Kahn, S. M., & Szymkowiak, A. E. 2006, Physical Review Letters, 96, 253201

Brown, G. V., Beiersdorfer, P., Liedahl, D. A., Widmann, K., & Kahn, S. M. 1998, ApJ, 502, 1015

Brown, G. V., Beiersdorfer, P., Liedahl, D. A., Widmann, K., Kahn, S. M., & Clothiaux, E. J. 2002, ApJS, 140, 589

Brown, G. V., Beiersdorfer, P., & Widmann, K. 2001b, Phys. Rev. A, 63, 032719

Chen, H., Gu, M. F., Beiersdorfer, P., Boyce, K. R., Brown, G. V., Kahn, S. M., Kelley, R. L., Kilbourne, C. A., Porter, F. S., & Scofield, J. H. 2006, ApJ, 646, 653

Desai, P., Brickhouse, N. S., Drake, J. J., Dupree, A. K., Edgar, R. J., Hoogerwerf, R., Kashyap, V., Wargelin, B. J., Smith, R. K., Huenemoerder, D. P., & Liedahl, D. A. 2005, ApJ, 625, L59

Gu, M. F. 2003, ApJ, 582, 1241

Gu, M. F., Beiersdorfer, P., Brown, G. V., Chen, H., rn, D. B. T., & Kahn, S. M. 2007, ApJ, 657, 1172

Gu, M. F., Gupta, R., Peterson, J. R., Sako, M., & Kahn, S. M. 2006, ApJ, 649, 979

Levine, M. A., Marrs, R. E., Henderson, J. R., Knapp, D. A., & Schneider, M. B. 1988, Physica Scripta Volume T, 22, 157

McKenzie, D. L., Landecker, P. B., Broussard, R. M., Rugge, H. R., Young, R. M., Feldman, U., & Doschek, G. A. 1980, ApJ, 241, 409

Parkinson, J. H. 1975, Sol. Phys., 42, 183

Phillips, K. J. H., Fawcett, B. C., Kent, B. J., Gabriel, A. H., Leibacher, J. W., Wolfson, C. J., Acton, L. W., Parkinson, J. H., Culhane, J. L., & Mason, H. E. 1982, ApJ, 256, 774

Phillips, K. J. H., Mewe, R., Harra-Murnion, L. K., Kaastra, J. S., Beiersdorfer, P., Brown, G. V., & Liedahl, D. A. 1999, A&AS, 138, 381

Saba, J. L. R., Schmelz, J. T., Bhatia, A. K., & Strong, K. T. 1999, ApJ, 510, 1064

Witthoeft, M. C., Badnell, N. R., del Zanna, G., Berrington, K. A., & Pelan, J. C. 2006, A&A, 446, 361

Xu, H., Kahn, S. M., Peterson, J. R., Behar, E., Paerels, F. B. S., Mushotzky, R. F., Jernigan, J. G., Brinkman, A. C., & Makishima, K. 2002, ApJ, 579, 600

Table 1. Comparison of experimental, theoretical, and observational line ratios of Fe XVIII.

Label[a]	Theory A[b]	Theory B[c]	Exp.	Theory C[d]	Theory D[e]	Capella [f]
F20	6.10[g]	5.58[g]	5.6(8)[g]	···	···	···
F1	0.34	0.32	0.29(3)	···	0.38	0.21
F2	0.042	0.052	0.043(6)	···	0.046	···
F3	0.17	0.16	0.16(2)	···	0.17	0.09
F4	0.41	0.48	0.60(6)	0.60	0.68	0.71
F5,6	0.31	0.36	0.44(5)	0.38[h]	0.44	0.58
F8	0.15	0.17	0.19(2)	0.13	0.21	0.24
F9	0.16	0.17	0.20(2)	0.23	0.21	0.21
F11	0.25	0.29	0.30(4)	0.34	0.31	0.31
F13,14,15	0.34	0.38	0.38(4)	0.34[h]	0.38	0.43
F16	0.10	0.10	0.09(1)	···	0.11	···
F17,18	0.37	0.39	0.33(4)	0.38	0.38	0.39
F19	0.20	0.22	0.20(2)	0.21	0.20	0.3

[a]Labels are from Brown et al. (2002).

[b]Theory with limited configuration interaction.

[c]Theory with more extensive configuration interaction.

[d]R-matrix theory of Witthoeft et al. (2006).

[e]Theory with resonance excitation and dielectronic recombination contributions from Gu (2003).

[f]*Chandra* MEG observations of Caplla from Desai et al. (2005).

[g]Line ratios are relative to the intensity of F20. The theoretical values tabulated for F20 are the total effective cross sections for forming this line in unit of 10^{-20} cm^2. The experimental formation cross section for F20 is from Chen et al. (2006). Numbers in the parentheses for the experimental values are the uncertainties in the last digit.

[h]Witthoeft et al. (2006) only gave the ratio for F6 and F15, the ratio for F5+F6 and F13+F14+F15 are derived by using the F5 to F6 and F13+F14 to F15 ratios of "Theory D".

Table 2. Comparison of experimental and theoretical line ratios of Ni XX.

Label[a]	Theory A[b]	Theory B[c]	Exp.
F20	4.5[d]	3.86[d]	...
F1	0.36	0.33	0.36(5)[d]
F2	0.06	0.07	0.08(2)
F3	0.16	0.15	0.13(2)
F4	0.44	0.46	0.58(8)
F5,6	0.32	0.36	0.42(6)
F8	0.14	0.17	0.20(3)
F9	0.14	0.16	0.18(3)
F11	0.23	0.27	0.26(4)
F13,14,15	0.44	0.50	0.55(7)
F16	0.17	0.17	0.17(3)
F17,18	0.39	0.41	0.40(6)
F19	0.21	0.23	0.21(4)[e]

[a]Labels are from Brown et al. (2002).

[b]Theory with limited configuration interaction.

[c]Theory with more extensive configuration interaction.

[g]Line ratios are relative to the intensity of F20. The theoretical values tabulated for F20 are the total effective cross sections for forming this line in unit of 10^{-20} cm^2. Numbers in the parentheses for the experimental values are the uncertainties in the last digit.

[e]The F20 and F19 lines of Ni XX are marginally resolved, the ratio of the two lines are fixed at the value predicted by theory A during the spectral fitting.

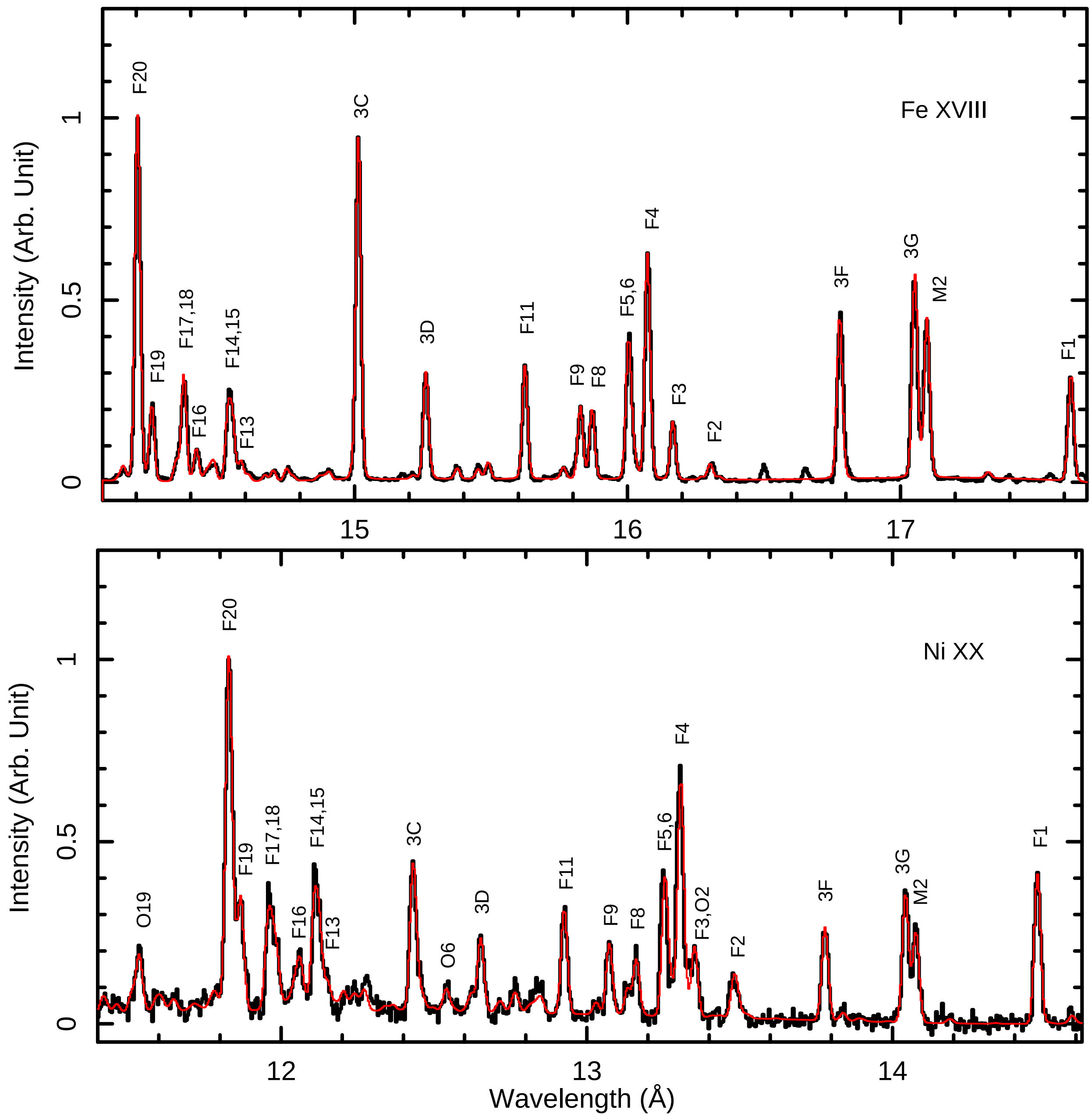

Fig. 1.— Measured spectra and model fits of Fe XVIII and Ni XX lines. Black and red traces are the data and models, respectively.

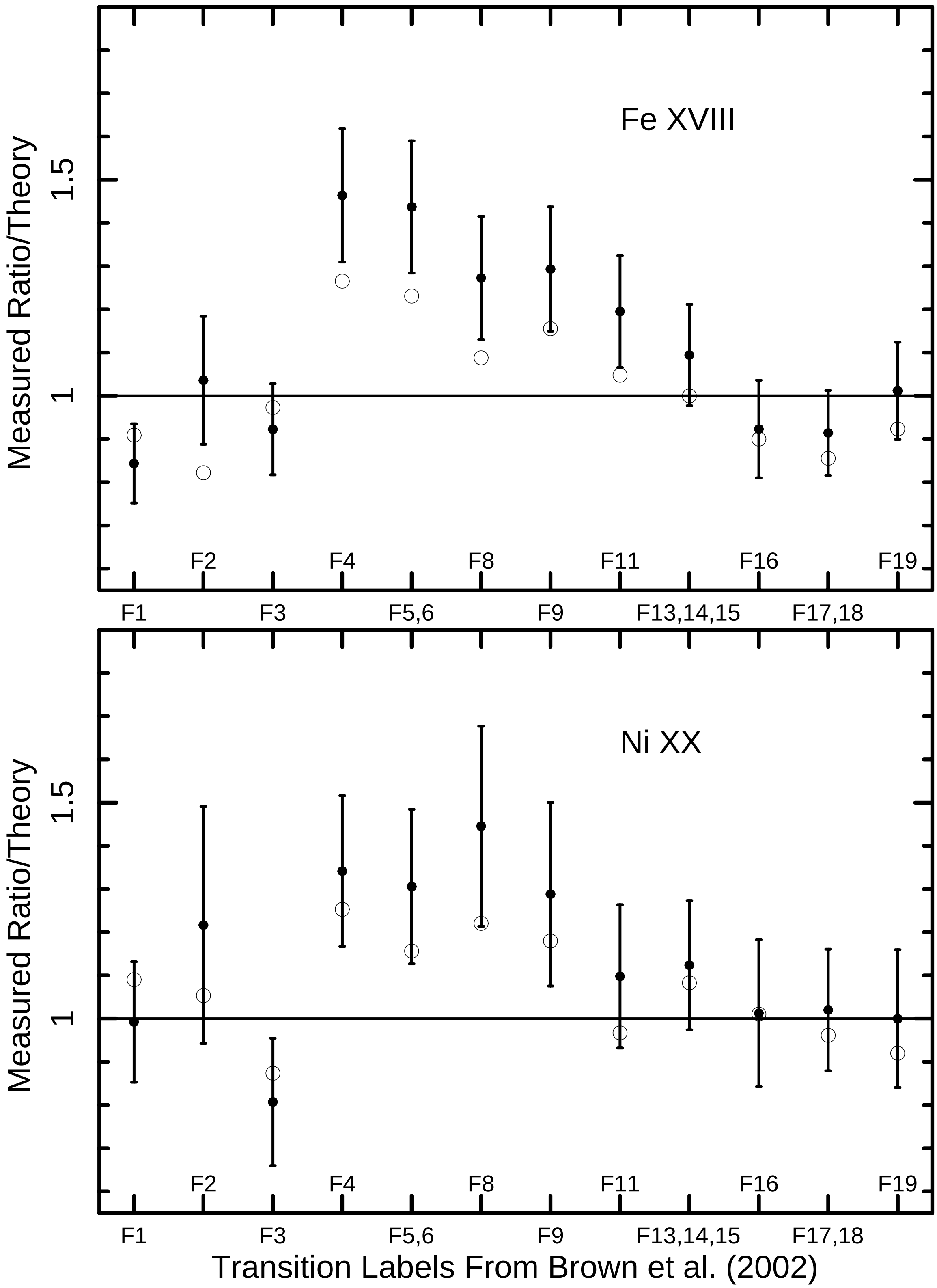

Fig. 2.— Comparison of theoretical and experimental line ratios of Fe XVIII and Ni XX. The filled circles are the ratios of measured to "Theory A" line intensities relative to that of the F20 line. The open circles are the ratios using "Theory B".